



## MAG-PGSTE: A new STE-based PGSE NMR sequence for the determination of diffusion in magnetically inhomogeneous samples

Gang Zheng, William S. Price\*

Nanoscale Organisation and Dynamics Group, College of Health and Science, University of Western Sydney, Penrith South DC, NSW 1797, Australia

### ARTICLE INFO

#### Article history:

Received 14 April 2008

Revised 5 August 2008

Available online 14 August 2008

#### Keywords:

Background gradients

Diffusion

Glass beads

Internal gradients

NMR

PGSE

Stimulated echo

### ABSTRACT

A new stimulated echo based pulsed gradient spin-echo sequence, MAG-PGSTE, has been developed for the determination of self-diffusion in magnetically inhomogeneous samples. The sequence was tested on two glass bead samples (i.e., 212–300 and <106  $\mu\text{m}$  glass bead packs). The MAG-PGSTE sequence was compared to the MAGSTE (or MPFG) [P.Z. Sun, J.G. Seland, D. Cory, Background gradient suppression in pulsed gradient stimulated echo measurements, *J. Magn. Reson.* 161 (2003) 168–173; P.Z. Sun, S.A. Smith, J. Zhou, Analysis of the magic asymmetric gradient stimulated echo sequence with shaped gradients, *J. Magn. Reson.* 171 (2004) 324–329; P.Z. Sun, Improved diffusion measurement in heterogeneous systems using the magic asymmetric gradient stimulated echo (MAGSTE) technique, *J. Magn. Reson.* 187 (2007) 177–183; P. Galvosas, F. Stallmach, J. Kärger, Background gradient suppression in stimulated echo NMR diffusion studies using magic pulsed field gradient ratios, *J. Magn. Reson.* 166 (2004) 164–173, P. Galvosas, PFG NMR-Diffusionsuntersuchungen mit ultra-hohen gepulsten magnetischen Feldgradienten an mikroporösen Materialien, Ph.D. Thesis, Universität Leipzig, 2003, P.Z. Sun, Nuclear Magnetic Resonance Microscopy and Diffusion, Ph.D. Thesis, Massachusetts Institute of Technology, 2003] sequence and Cotts 13-interval [R.M. Cotts, M.J.R. Hoch, T. Sun, J.T. Marker, Pulsed field gradient stimulated echo methods for improved NMR diffusion measurements in heterogeneous systems, *J. Magn. Reson.* 83 (1989) 252–266] sequence using both glass bead samples. The MAG-PGSTE and MAGSTE (or MPFG) sequences outperformed the Cotts 13-interval sequence in the measurement of diffusion coefficients; more interestingly, for the sample with higher background gradients (i.e., the <106  $\mu\text{m}$  glass bead sample), the MAG-PGSTE sequence provided higher signal-to-noise ratios and thus better diffusion measurements than the MAGSTE and Cotts 13-interval sequences. In addition, the MAG-PGSTE sequence provided good characterization of the surface-to-volume ratio for the glass bead samples.

© 2008 Elsevier Inc. All rights reserved.

### 1. Introduction

It has long been realized that the existence of background gradients (also referred to as internal gradients or static gradients ( $g_0$ )) caused by the imperfect shimming of  $\mathbf{B}_0$  and/or differences in magnetic susceptibility both within and around the sample can cause deleterious effects on the determination of self-diffusion [8]. Therefore, background gradient suppression pulsed gradient spin-echo (PGSE) sequences have been intensively studied [7,9–27] and this area has recently been reviewed by Zheng and Price [14]. With short exposure (i.e., encoding periods ( $\tau_e$ )) to background gradients and transverse relaxation, stimulated echo (STE,  $\pi/2-\tau_e-\pi/2-\tau_s-\pi/2-\tau_e$ -Echo) based PGSE sequences outperform Hahn spin-echo based PGSE sequences in the presence of background gradients due to their lower susceptibility to the attenuation by background gradients, and to the attenuation by transverse relaxation. In 1989, Cotts et al. [7] developed the

so-called 9-interval, 13-interval (Fig. 1A), and 17-interval STE-based background gradient suppression PGSE sequences. Owing to the use of bipolar gradient pairs, the 13-interval and 17-interval sequences and their derivatives afford longer gradient application periods, and thus find wide applications in diffusion experiments on magnetically inhomogeneous samples [19–21,24].

Up to now, most of the background gradient suppression sequences are based on the assumption that the background gradient experienced by each spin is constant during the PGSE sequence, and  $\pi$  pulse trains and bipolar gradient pairs have been utilized in these sequences to suppress the effects of background gradients. However, when the mean-squared-displacement (MSD) of the spins during the PGSE experiment becomes comparable with the length scale of the inhomogeneity of background gradients, the background gradient experienced by each spin becomes non-constant both spatially and temporally [24,28,29]. By replacing the initial symmetric bipolar gradient pairs by asymmetric bipolar gradient pairs, Sun et al. [1–3,6] and Galvosas et al. [4,5] independently modified the 13-interval sequence into a series of STE-based PGSE sequences (i.e., MAGSTE or MPFG sequences) containing

\* Corresponding author. Fax: +61 2 4620 3025.

E-mail address: [w.price@uws.edu.au](mailto:w.price@uws.edu.au) (W.S. Price).

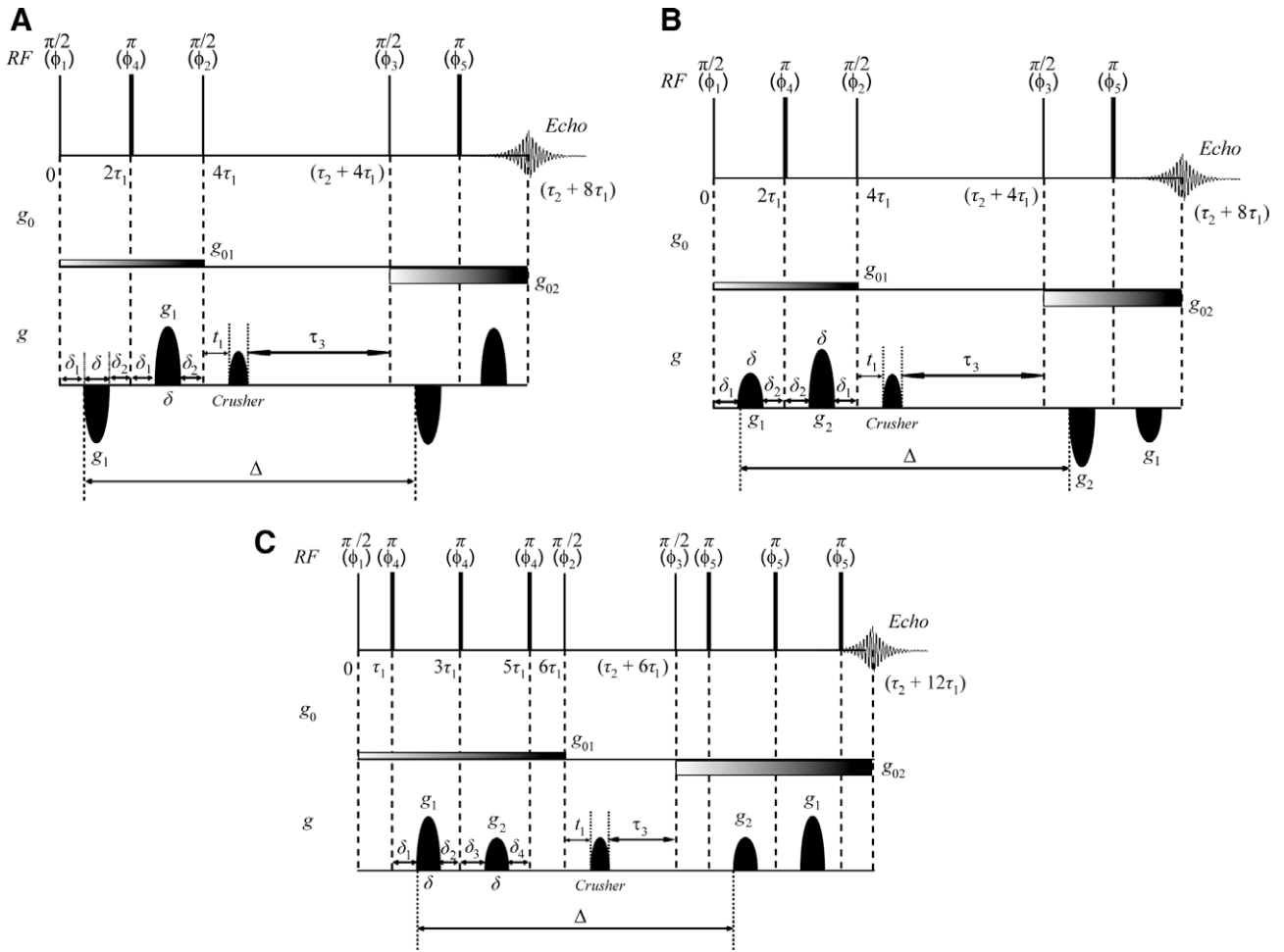


**Fig. 1.** (A) The Cotts 13-interval sequence [7] with half-sine shaped gradients. The phase cycle for the pulse sequence is  $\phi_1 = x$ ;  $\phi_2 = x, y, -x, -y$ ;  $\phi_3 = x, y, -x, -y, -x, -y, x, y$ ;  $\phi_4 = x$ ;  $\phi_5 = x, y, -x, -y, -x, -y, x, y$ ;  $\phi_r$  (receiver phase) =  $-x, x, -x, x, x, -x, x, -x$ . (B) The MAGSTE sequence with half-sine shaped gradients [2]. The phase cycle for the pulse sequence is  $\phi_1 = x$ ;  $\phi_2 = x, -x, x, -x, y, -y, y, -y$ ;  $\phi_3 = x, x, -x, -x, y, y, -y, -y$ ;  $\phi_4 = y$ ;  $\phi_5 = y$ ;  $\phi_r$  (receiver phase) =  $x, -x, -x, x$ . (C) The MAG-PGSTE sequence with half-sine shaped gradients. The phase cycle for the pulse sequence is  $\phi_1 = x$ ;  $\phi_2 = x, -x, x, -x, y, -y, y, -y$ ;  $\phi_3 = x, x, -x, -x, y, y, -y, -y$ ;  $\phi_4 = y$ ;  $\phi_5 = y, y, -y, -y, -x, -x, x, x$ ;  $\phi_r$  (Receiver phase) =  $x, -x, -x, x$ . The narrow bars represent  $\pi/2$  and  $\pi$  RF pulses,  $g_{01}$  and  $g_{02}$  are background gradients,  $g_1$ ,  $g_2$  and crusher are half-sine shaped gradient pulses with different amplitudes. The variable gradient fill for  $g_{01}$  and  $g_{02}$  signifies that the background gradients may fluctuate during the encoding periods.

asymmetric gradient pairs with the amplitudes of the gradient pulses set at “magic” ratios (i.e., the gradient amplitude ratios which result in zero cross-term between applied and background gradients), and these sequences can suppress the effects of non-constant background gradients in one transient (e.g. Fig. 1B). For the 13-interval sequence, the cross-term generated in the first encoding period is cancelled by the cross-term generated in the second encoding period with appropriate parameter settings (i.e.,  $E_{\text{cross}} \neq 0$  at the end of the first encoding period and  $E_{\text{cross}} = 0$  at the end of the second encoding period;  $E_{\text{cross}}$  is the cross-term based spin-echo attenuation.) [7,14]; while for the MAGSTE or MPFG sequence, the cross-terms generated in the two encoding periods are suppressed independently (i.e.,  $E_{\text{cross}} = 0$  at the end of the first or second encoding period) [1,4].

It has been shown that the 17-interval sequence outperforms the 13-interval sequence in the suppression of the  $g_0$ -only-based attenuation ( $E_{g_0}$ ), which becomes very significant in the presence of high background gradients [7]. Therefore, a new STE-based PGSE sequence, MAG-PGSTE (Fig. 1C), which can suppress the effects of non-constant background gradients with a higher signal-to-noise (S/N) ratio, was developed by replacing the symmetric bipolar gradient pairs in the 17-interval sequence by asymmetric bipolar gradient pairs with the gradient amplitudes set at the “magic” ratio

[1,4]. The utility of the new sequence is demonstrated using two samples containing glass bead packs (NB with bead diameters 212–300 and  $<106 \mu\text{m}$ ) filled with  $\text{CuSO}_4$ -doped water. The performance of the new sequence was contrasted with the MAGSTE and Cotts 13-interval sequences.

## 2. Theory

In many samples the background gradients can approach the magnitude of the applied gradients. For example, the background gradients in the 212–300 and  $<106 \mu\text{m}$  glass bead samples have been estimated to be 0.2 and  $1.1 \text{ T m}^{-1}$  (e.g. [24]), respectively, which are comparable to the maximum gradient strength of a commercial high-resolution gradient NMR probe (e.g.  $0.6 \text{ T m}^{-1}$ ), and thus can cause a poor S/N ratio. Therefore, more  $\pi$  pulses are needed in the encoding periods to minimize the attenuation caused by the background gradients and thus increase the S/N ratio. This thinking led to the development of the MAG-PGSTE sequence by integrating asymmetric bipolar gradient pairs with the Cotts 17-interval sequence [7] containing three- $\pi$ -pulse CPMG train [10] in each encoding period.

Following Stejskal and Tanner analysis based on solving the Bloch–Torrey equations [8], the applied gradients based echo

attenuation ( $E_g$ ),  $E_{\text{cross}}$ , and  $E_{g_0}$  of the MAG-PGSTE sequence with half-sine shaped gradients (Fig. 1C) for free diffusion are derived as

$$E_g = \exp \left\{ -\frac{1}{\pi^2} \gamma^2 \delta^2 D \left[ (4\Delta + 8\tau_1 - \delta + 4\delta_3 - 4\delta_1)(g_1 - g_2)^2 + (32\tau_1 - 2\delta + 16\delta_3 - 16\delta_1)(g_1 - g_2)g_2 + (16\tau_1 - 2\delta + 8\delta_3 - 8\delta_1)g_2^2 \right] \right\} = \exp(-b_g D), \quad (1)$$

$$E_{\text{cross}} = \exp \left\{ -\frac{1}{\pi^2} \gamma^2 \delta g_1 D \left[ g_{01} (\eta (4\delta^2 - \pi^2 \delta^2 + 2\pi^2 \tau_1^2 + 4\pi^2 \tau_1 \delta_3 - 2\pi^2 \delta_3^2 + 2\pi^2 \tau_1 \delta - 2\pi^2 \delta \delta_3) - (\pi^2 \delta^2 + 2\pi^2 \delta \delta_1 - 2\pi^2 \tau_1 \delta - 4\delta^2 + 2\pi^2 \tau_1^2 - 4\pi^2 \tau_1 \delta_1 + 2\pi^2 \delta_1^2)) + g_{02} (\eta (-4\delta^2 + \pi^2 \delta^2 - 2\pi^2 \tau_1^2 - 4\pi^2 \tau_1 \delta_1 + 2\pi^2 \delta_1^2 - 2\pi^2 \tau_1 \delta + 2\pi^2 \delta \delta_1) + (\pi^2 \delta^2 + 2\pi^2 \delta \delta_3 - 2\pi^2 \tau_1 \delta - 4\delta^2 + 2\pi^2 \tau_1^2 - 4\pi^2 \tau_1 \delta_3 + 2\pi^2 \delta_3^2)) \right] \right\} = \exp(-b_{\text{cross}} D), \quad (2)$$

where  $\eta = g_2/g_1$ , and

$$E_{g_0} = \exp[-2\gamma^2 \tau_1^3 D (g_{01}^2 + g_{02}^2)] = \exp(-b_{g_0} D). \quad (3)$$

For Eqs. (1)–(3),  $g_1$ ,  $g_2$ ,  $g_{01}$ ,  $g_{02}$ , and the timing parameters are defined in Fig. 1C.

In general, we are concerned with the strong background gradients in porous media where measured diffusion coefficients become time-dependent due to the existence of geometrical restrictions. The time-dependence of the measured diffusion coefficients carries structural information of the porous media. At short diffusion times, the time-dependent diffusion coefficient ( $D(\Delta)$ ) is defined as [30,31]

$$D(\Delta) = D_0 \left[ 1 - \frac{4}{9\sqrt{\pi}} \frac{S}{V} \sqrt{D_0 \Delta} + O(D_0 \Delta) \right], \quad (4)$$

where  $D_0$  is the free diffusion coefficient,  $S/V$  is the surface-to-volume ratio.

Including the time-dependence of measured diffusion coefficients, Eqs. (1)–(3) can be rewritten as [18,19,30]

$$E_g = \exp(-b_g D(\Delta)), \quad (5)$$

$$E_{\text{cross}} = \exp(-b_{\text{cross}} D(\Delta)), \quad (6)$$

and

$$E_{g_0} = \exp(-b_{g_0} D(\Delta)). \quad (7)$$

By solving  $b_{\text{cross}} = 0$  for  $\eta$  when  $\delta_1 = \delta_3$  or  $\delta_2 = \delta_3$ , the magic gradient amplitude ratio for suppressing the cross-terms between the applied and background gradients is determined to be

$$\eta_{\text{MAG-PGSTE}} = \frac{2\tau_1^2 - (2\delta\tau_1 + 4\delta_1\tau_1 - \delta^2 - 2\delta\delta_1 - 2\delta_1^2 + 4\delta^2/\pi^2)}{2\tau_1^2 + (2\delta\tau_1 + 4\delta_1\tau_1 - \delta^2 - 2\delta\delta_1 - 2\delta_1^2 + 4\delta^2/\pi^2)}. \quad (8)$$

To assure the validity of Eqs. (1)–(3) in our data analysis, the maximum echo attenuation was controlled to be 80% (i.e., 20% of the original intensity remaining) in all data analysis and the condition, namely  $qL \gg 1$  ( $q = (2\pi)^{-1} \gamma g \delta$  and  $L$  is the length of the sample), was also fulfilled by setting the minimum gradient strength to  $0.005 \text{ T m}^{-1}$  in all our experiments [20].

### 3. Materials and methods

Micro-spherical acid-washed glass beads with sizes of <106 and 212–300  $\mu\text{m}$  (Sigma-Aldrich Inc., St. Louis, MO) were transferred into two 5 mm NMR tubes (Wilmad, Buena, NJ) filled with 0.01 M  $\text{CuSO}_4 \cdot 5\text{H}_2\text{O}$  solution. Another 5 mm NMR tube containing 0.01 M  $\text{CuSO}_4 \cdot 5\text{H}_2\text{O}$  solution was used as a reference sample. The diffusion coefficient of water in the reference sample was found to be  $2.33 \pm 0.01 \times 10^{-9} \text{ m}^2 \text{ s}^{-1}$  at 25 °C using the standard Hahn spin-echo PGSE sequence.

All diffusion measurements were conducted ‘unlocked’ on a Bruker 500 MHz Avance NMR spectrometer (Karlsruhe, Germany) with a BBI probe at 25 °C. By using the MAG-PGSTE and Cotts 13-interval [7] sequence with half-sine shaped gradients, diffusion measurements were conducted with  $\tau_2 = 3.05, 5.05, 7.05, 10.05, 15.05, 22.05, 31.05, 46.05, 63.05, 91.05, 127.05, 255.05, 511.05$  ms; by using the MAGSTE [1] sequence with half-sine shaped gradients, diffusion measurements were conducted with  $\tau_2 = 7.05, 10.05, 15.05, 22.05, 31.05, 46.05, 63.05, 91.05, 127.05, 255.05, 511.05$  ms. For all diffusion measurements,  $\delta = 3$  ms,  $\tau_e = 10$  ms, recycle delay = 5 s ( $\text{NB} > 5 \times T_1$ ), and number of scans = 8. The delays are defined in Fig. 1. Each diffusion measurement involved 21 z-gradient strengths (e.g.  $g_1$  for the MAG-PGSTE and Cotts 13-interval sequence and  $g_2$  for the MAGSTE sequence) that varied linearly from  $0.005 \text{ T m}^{-1}$  to the value which gave an attenuation of 80–90%.

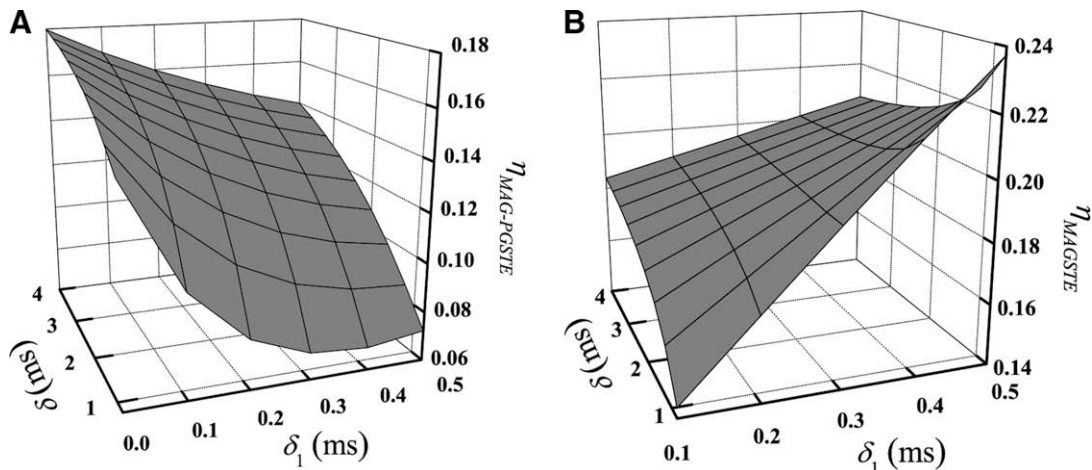
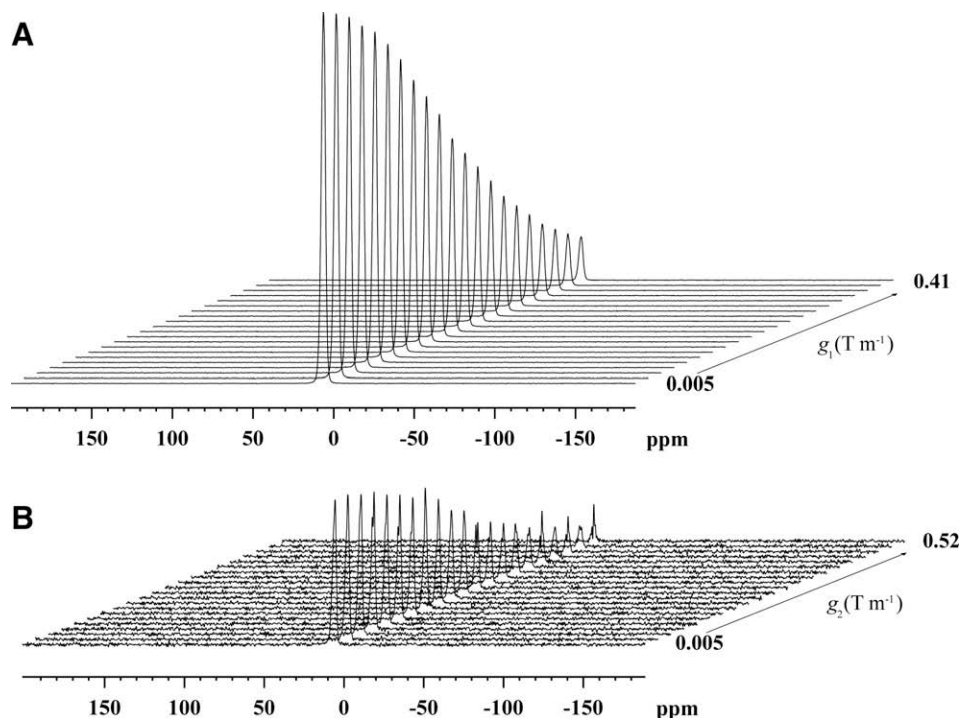


Fig. 2. (A) The magic ratio for the MAG-PGSTE sequence when  $\delta_2 = 0.2$  ms,  $\delta_1$  ranging from 0 to 0.5 ms, and  $\delta$  ranging from 0.8 to 4 ms. (B) The magic ratio for the MAGSTE sequence when  $\delta_2 = 0.2$  ms,  $\delta_1$  ranging from 0 to 0.5 ms, and  $\delta$  ranging from 0.8 to 4 ms.



**Fig. 3.** A series of 500 MHz  $^1\text{H}$  (A) MAG-PGSTE and (B) MAGSTE spectra on the sample containing  $\text{CuSO}_4$ -doped water and  $<106\ \mu\text{m}$  glass beads. For both sequences,  $\delta = 3\ \text{ms}$ ,  $\tau_e = 10\ \text{ms}$ ,  $\Delta = 41\ \text{ms}$ , receiver gain = 128 (MAG-PGSTE) and 812 (MAGSTE). As can be clearly seen the MAG-PGSTE spectra have much higher S/N.

All data were processed using Origin (OriginLab, Northampton, MA). The time-dependent diffusion coefficient was determined from fitting the single-exponential equation  $y = Me^{-b_g D(\Delta)}$  ( $M$  is a constant,  $b_g$  and  $D(\Delta)$  are defined in Eqs. (1) and (4), respectively.) to the echo attenuation profiles.

#### 4. Results and discussion

For the MAGSTE sequence developed by Sun et al. [1], the cross-term caused by non-constant background gradients can be suppressed, only when the bipolar gradients are symmetrically placed around  $\pi$  pulses. However, for the newly developed MAG-PGSTE sequence, a unique magic ratio (i.e.,  $\eta_{\text{MAG-PGSTE}} = g_2/g_1$ ) has been obtained for the suppression of the cross-term when  $\delta_1 = \delta_3$  or  $\delta_2 = \delta_3$ . Especially, when  $\delta_1 = \delta_3$ , both  $\delta_1$  and  $\delta_3$  can be set as small as possible to minimize eddy current effects. The MPFG sequence also has this property [4].

Based on the simulations, the MAG-PGSTE sequence has a magic ratio ( $\eta_{\text{MAG-PGSTE}}$ ) smaller than the magic ratio for the MAGSTE sequence ( $\eta_{\text{MAGSTE}}$ ), and thus giving higher applied gradient encoding efficiency. As shown in Fig. 2A, when  $\delta_2 = 0.2\ \text{ms}$ ,  $\delta_1$  ranging from 0 to 0.5 ms, and  $\delta$  ranging from 0.8 to 4 ms,  $\eta_{\text{MAG-PGSTE}}$  ranges from 0.07 to 0.18; while, in Fig. 2B, when  $\delta_2 = 0.2\ \text{ms}$ , with  $\delta_1$  ranging from 0.2 to 0.5 ms, and  $\delta$  ranging from 0.8 to 4 ms,  $\eta_{\text{MAGSTE}}$  ranges from 0.17 to 0.24.

As shown in Fig. 3, for the  $<106\ \mu\text{m}$  glass bead sample, the MAG-PGSTE spectra had a much better S/N ratio than the MAGSTE spectra.

The utility of the MAG-PGSTE sequence has been demonstrated on glass bead packs filled with  $\text{CuSO}_4\text{-}5\text{H}_2\text{O}$  solution. To show the dependence of  $D(\Delta)$  on  $\Delta$ ,  $D(\Delta)$  was plotted against  $\Delta$  (Fig. 4). As shown in Fig. 4, all diffusion measurements were lower than the diffusion coefficient of water in the reference sample (i.e.,  $2.33 \pm 0.01 \times 10^{-9}\ \text{m}^2\ \text{s}^{-1}$ ) due to the effects of highly intense and inhomogeneous background gradients [3,11,28,29,32], which is analogous to the apparent slowing down of diffusion in pores with

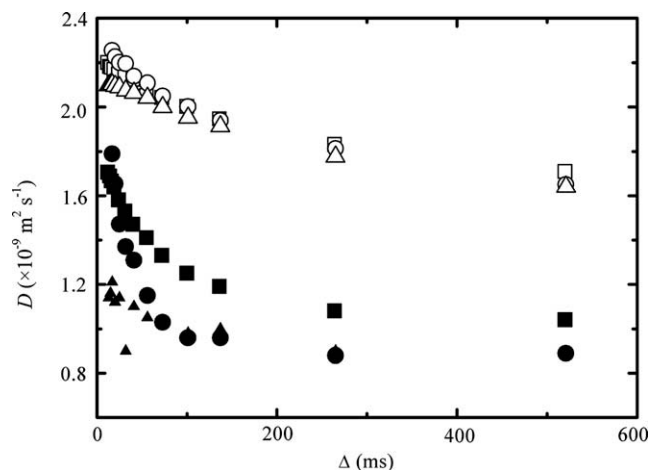


**Fig. 4.** A plot of  $D(\Delta)$  vs.  $\Delta$  for the diffusion measurements of  $<106$  and  $212\text{--}300\ \mu\text{m}$  glass bead samples are shown in solid and open symbols, respectively. The data obtained with the MAG-PGSTE, MAGSTE, and Cotts 13-interval sequence are indicated by squares, circles, and triangles, respectively.

relaxing boundaries [33]. For the  $<106\ \mu\text{m}$  glass bead sample, the MAG-PGSTE sequence consistently gave higher diffusion measurements owing to its high efficiency in the suppression of both  $E_{\text{cross}}$  and  $E_{g_0}$  except that the MAGSTE sequence gave the highest diffusion measurement when  $\Delta = 17.05\ \text{ms}$ . For the  $212\text{--}300\ \mu\text{m}$  glass bead sample, the MAGSTE sequence consistently gave higher diffusion measurements at short diffusion times (i.e.,  $\leq 100\ \text{ms}$ ) due to its higher efficiency in the suppression of  $E_{\text{cross}}$  while, at long diffusion times, the MAGSTE diffusion measurements overlapped with the MAG-PGSTE and Cotts 13-interval diffusion measurements.

To test the sphere size characterization capability of the MAG-PGSTE sequence, Eq. (4) was fitted to the diffusion measurements at short diffusion times (i.e.,  $\leq 100\ \text{ms}$ ), and the measured bead diameters and S/V's are shown in Table 1. The measured bead

**Table 1**

Bead diameters and  $S/V$ 's of the glass bead samples determined from data obtained with the MAG-PGSTE, MAGSTE, and Cotts 13-interval sequence

Sequence	Sample	Measured diameter ( $\mu\text{m}$ )	$S/V$ ( $\mu\text{m}^{-1}$ )
MAG-PGSTE	<106 $\mu\text{m}$ beads	93	$0.105 \pm 0.007$
	212–300 $\mu\text{m}$ beads	280	$0.035 \pm 0.002$
MAGSTE	<106 $\mu\text{m}$ beads	61	$0.16 \pm 0.02$
	212–300 $\mu\text{m}$ beads	218	$0.045 \pm 0.002$
Cotts 13-interval	<106 $\mu\text{m}$ beads	122	$0.08 \pm 0.03$
	212–300 $\mu\text{m}$ beads	350	$0.028 \pm 0.002$

$S/V$ 's were obtained by fitting Eq. (4) to the diffusion data at short diffusion times (i.e.,  $\leq 100$  ms) and the measured bead diameters were calculated by the use of  $d = 6(1/\phi - 1)/S/V$  [19] with a porosity of  $\phi = 0.38$  (e.g. [19]).

diameters using the MAG-PGSTE and MAGSTE sequence matched the nominal bead diameters very well. Although the Cotts 13-interval sequence can differentiate between the two glass bead samples, it over-estimated the bead diameters for both glass bead samples.

## 5. Conclusions

Due to its higher efficiency in suppressing both  $E_{\text{cross}}$  and  $E_{g_0}$ , the MAG-PGSTE sequence outperformed the MAGSTE and Cotts 13-interval sequence in diffusion measurements at different diffusion times in the presence of large and highly inhomogeneous background gradients in a glass bead sample composed of <106  $\mu\text{m}$  glass beads. The MAG-PGSTE sequence also provided accurate sphere size and  $S/V$  measurements for both glass bead samples.

## Acknowledgments

This research was supported by an Endeavour International Postgraduate Research Scholarship from the University Western Sydney and the Australian government (G.Z.), and a NSW BioFirst Award from the NSW Ministry for Science & Medical Research (W.S.P.).

## References

- [1] P.Z. Sun, J.G. Seland, D. Cory, Background gradient suppression in pulsed gradient stimulated echo measurements, *J. Magn. Reson.* 161 (2003) 168–173.
- [2] P.Z. Sun, S.A. Smith, J. Zhou, Analysis of the magic asymmetric gradient stimulated echo sequence with shaped gradients, *J. Magn. Reson.* 171 (2004) 324–329.
- [3] P.Z. Sun, Improved diffusion measurement in heterogeneous systems using the magic asymmetric gradient stimulated echo (MAGSTE) technique, *J. Magn. Reson.* 187 (2007) 177–183.
- [4] P. Galvosas, F. Stallmach, J. Kärger, Background gradient suppression in stimulated echo NMR diffusion studies using magic pulsed field gradient ratios, *J. Magn. Reson.* 166 (2004) 164–173.
- [5] P. Galvosas, PFG NMR-Diffusionsuntersuchungen mit ultra-hohen gepulsten magnetischen Feldgradienten an mikroporösen Materialien, Ph.D. Thesis, Universität Leipzig, 2003.
- [6] P.Z. Sun, Nuclear Magnetic Resonance Microscopy and Diffusion, Ph.D. Thesis, Massachusetts Institute of Technology, 2003.
- [7] R.M. Cotts, M.J.R. Hoch, T. Sun, J.T. Marker, Pulsed field gradient stimulated echo methods for improved NMR diffusion measurements in heterogeneous systems, *J. Magn. Reson.* 83 (1989) 252–266.
- [8] E.O. Stejskal, J.E. Tanner, Spin diffusion measurements: spin echoes in the presence of a time-dependent field gradient, *J. Chem. Phys.* 42 (1965) 288–292.
- [9] X. Zhang, C.G. Li, C.H. Ye, M.L. Liu, Determination of molecular self-diffusion coefficient using multiple spin-echo NMR spectroscopy with removal of convection and background gradient artifacts, *Anal. Chem.* 73 (2001) 3528–3534.
- [10] S. Meiboom, D. Gill, Modified spin-echo method for measuring nuclear relaxation times, *Rev. Sci. Instrum.* 29 (1958) 688–691.
- [11] J. Kärger, H. Pfeifer, W. Heink, Principles and application of self-diffusion measurements by nuclear magnetic resonance, *Adv. Magn. Reson.* 12 (1988) 1–89.
- [12] W.S. Price, Pulsed-field gradient nuclear magnetic resonance as a tool for studying translational diffusion: part II. Experimental aspects, *Concepts Magn. Reson.* 10A (1998) 197–237.
- [13] F. Stallmach, P. Galvosas, Spin echo NMR diffusion studies, *Annu. Rep. NMR Spectrosc.* 61 (2007) 51–131.
- [14] G. Zheng, W.S. Price, Suppression of background gradients in ( $B_0$  gradient-based) NMR diffusion experiments, *Concepts Magn. Reson.* 30A (2007) 261–277.
- [15] H.Y. Carr, E.M. Purcell, Effects of diffusion on free precession in nuclear magnetic resonance experiments, *Phys. Rev.* 94 (1954) 630–638.
- [16] W.D. Williams, E.F.W. Seymour, R.M. Cotts, A pulsed-gradient multiple-spin-echo NMR technique for measuring diffusion in the presence of background magnetic field gradients, *J. Magn. Reson.* 31 (1978) 271–282.
- [17] R.F. Karlicek Jr., I.J. Lowe, A modified pulsed gradient technique for measuring diffusion in the presence of large background gradients, *J. Magn. Reson.* 37 (1980) 75–91.
- [18] L.L. Latour, L.M. Li, C.H. Sotak, Improved PFG stimulated-echo method for the measurement of diffusion in inhomogeneous fields, *J. Magn. Reson. B* 101 (1993) 72–77.
- [19] L.L. Latour, P.P. Mitra, R.L. Kleinberg, C.H. Sotak, Time-dependent diffusion coefficient of fluids in porous media as a probe of surface-to-volume ratio, *J. Magn. Reson. A* 101 (1993) 342–346.
- [20] M.D. Hürlimann, K.G. Helmer, L.L. Latour, C.H. Sotak, Restricted diffusion in sedimentary rocks. Determination of surface-area-to-volume ratio and surface relaxivity, *J. Magn. Reson. A* 111 (1994) 169–178.
- [21] G.H. Sørland, B. Hafskjold, O. Herstad, A stimulated-echo method for diffusion measurements in heterogeneous media using pulsed field gradients, *J. Magn. Reson.* 124 (1997) 172–176.
- [22] G.H. Sørland, D. Aksnes, L. Gjerdåker, A pulsed field gradient spin-echo method for diffusion measurements in the presence of internal gradients, *J. Magn. Reson.* 137 (1999) 397–401.
- [23] M. Schachter, M.D. Does, A.W. Anderson, J.C. Gore, Measurements of restricted diffusion using an oscillating gradient spin-echo sequence, *J. Magn. Reson.* 147 (2000) 232–237.
- [24] J.G. Seland, G.H. Sørland, K. Zick, B. Hafskjold, Diffusion measurements at long observation times in the presence of spatially variable internal magnetic field gradients, *J. Magn. Reson.* 146 (2000) 14–19.
- [25] A. Duh, A. Mohorič, J. Stepišnik, I. Serša, The elimination of magnetic susceptibility artifacts in the micro-image of liquid–solid interfaces: internal gradient modulation by the CPMG RF train, *J. Magn. Reson.* 160 (2003) 47–51.
- [26] A. Mohorič, A modified PGSE for measuring diffusion in the presence of static magnetic field gradients, *J. Magn. Reson.* 174 (2005) 223–228.
- [27] J. Finsterbusch, Improved diffusion-weighting efficiency of pulsed gradient stimulated echo MR measurements with background gradient cross-term suppression, *J. Magn. Reson.* 191 (2008) 282–290.
- [28] I. Zupančič, Effect of the background gradients on PGSE NMR diffusion measurements, *Solid State Commun.* 65 (1988) 199–200.
- [29] J. Zhong, J.C. Gore, Studies of restricted diffusion in heterogeneous media containing variations in susceptibility, *Magn. Reson. Med.* 19 (1991) 276–284.
- [30] P.P. Mitra, P.N. Sen, L.M. Schwartz, Short-time behavior of the diffusion coefficient as a geometrical probe of porous media, *Phys. Rev. B Condens. Matter* 47 (1993) 8565–8574.
- [31] P.N. Sen, Time-dependent diffusion coefficient as a probe of geometry, *Concepts Magn. Reson.* 23A (2004) 1–21.
- [32] S. Vasenkov, P. Galvosas, O. Geier, N. Nestle, F. Stallmach, J. Kärger, Determination of genuine diffusivities in heterogeneous media using stimulated echo pulsed field gradient NMR, *J. Magn. Reson.* 149 (2001) 228–233.
- [33] A.V. Barzykin, K. Hayamizu, W.S. Price, M. Tachiya, Pulsed-Field-Gradient NMR of diffusive transport through a spherical interface into an external medium containing a relaxation agent, *J. Magn. Reson.* 114A (1995) 39–46.